

AN ELECTRON BOMBARDMENT FURNACE
FOR VAPOR PRESSURE STUDIES.
THE VAPOR PRESSURE
OF GOLD

By

JAMES EDWARD BENNETT


Bachelor of Science
Northwestern State College
Alva, Oklahoma
1957

Submitted to the Faculty of the Graduate School
of the Oklahoma State University
in partial fulfillment of the requirements
for the degree of
MASTER OF SCIENCE
May, 1962

NOV 6 1962

AN ELECTRON BOMBARDMENT FURNACE
FOR VAPOR PRESSURE STUDIES.
THE VAPOR PRESSURE
OF GOLD

Thesis Approved:


Thesis Advisor




Dean of the Graduate School

504264

ACKNOWLEDGEMENT

Indebtedness is acknowledged to Dr. R. D. Freeman for his close attention to and welcome interest in the efforts reported here.

Too, the author expresses his appreciation to the Oklahoma State University Research Foundation and to the Air Force Office of Scientific Research for financial assistance.

TABLE OF CONTENTS

Part		Page
I.	INTRODUCTION	1
II.	APPARATUS	2
	The Power Supply.	2
	The Electron Bombardment Furnace.	3
	Discussion.	16
	Auxillary Apparatus	20
III.	EXPERIMENTAL	22
	Performance of the Furnace.	22
	Discussion.	23
	Vapor Pressure Calculations	27
	Results	29
IV.	BIBLIOGRAPHY	45

LIST OF TABLES

Table	Page
I. Knudsen Cell Constants	8
II. Typical Control Values	26
III. Vapor Pressure of Gold	30
IV. X-ray Diffraction Data	37
V. Heat of Sublimation of Gold	42
VI. Summary of ΔH_{298}^0 for Gold	44

LIST OF FIGURES

Figure	Page
1. Relay Modification	4
2. Electron Bombardment Furnace	5
3. The Cell-block Assembly	6
4. Ceramic Ring with Insulated Connections	10
5. The Radiation Shielding Arrangement	12
6. Cell-block Geometries	19
7. Typical Heating Curves	24
8. Vapor Pressure of Gold	31
9. Sketch of Patterns Observed on the Surface of Gold Sample	35
10. Vapor Pressure of Gold	38
11. Graphical Summary of Available Information on the Vapor Pressure of Gold	41

INTRODUCTION

The purpose of the investigations reported here was two-fold: first, the construction of a high temperature electron bombardment furnace suitable for vapor pressure studies via the Knudsen method (16); second, the determination of the vapor pressure of gold with subsequent calculation of its heat of sublimation at 298.15°K .

The author hopes that an accurate description of the furnace and of the vapor pressure studies resulting from this work will prove useful in some positive manner to those whose concern is the investigation of systems at elevated temperatures.

PART II
APPARATUS

The Power Supply.

Heating by electron bombardment involves the acceleration of electrons through a potential field to a target. The bombarding electrons usually are obtained from the surface of a filament as the result of thermionic emission. The target of the bombardment current can be heated to extremely high temperatures if a sufficient driving force (the potential field) is available.

To assure a bombardment current composed of high energy electrons, or, which is effectively the same, to prevent the electrons from colliding with gas molecules and producing a gaseous discharge, electron bombardment heating must be done in vacuum.

Heating in vacuum also lessens the oxidation of furnace components, especially the refractory metals such as tungsten, molybdenum, and tantalum. Suitable vacuum conditions for bombardment heating are discussed in the section describing the vacuum system.

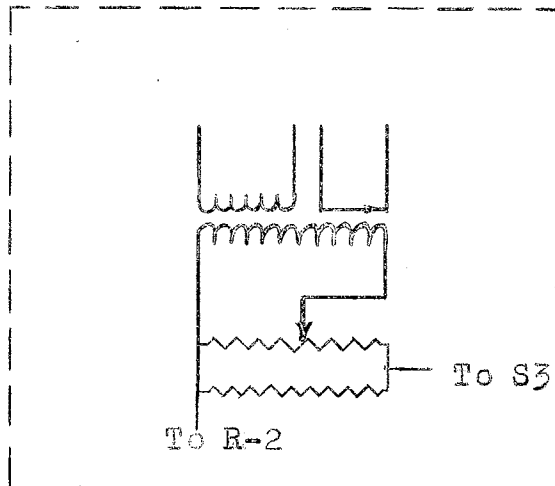
A power supply, constructed by Dawson (4), provides 3.0 KVA with output variable over the ranges 0-3000 VDC and 0-1000 ma. The filament is heated by low voltage A. C. current to temperatures sufficient for thermionic emission.

Dawson's power supply was found to function satisfactorily for this work, and his circuit diagram requires no change except for the following detail: the circuitry of Relay-2, page 5, Dawson's thesis (4), has been altered as shown in Figure 1, in which Dawson's notation is retained.

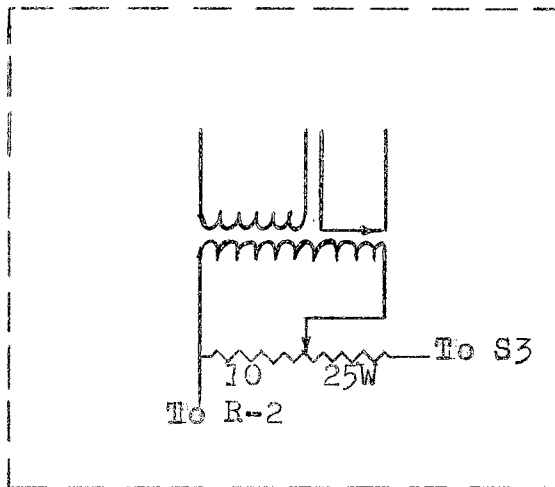
The Electron Bombardment Furnace.

Figure 2 gives a non-detailed drawing of the electron bombardment furnace, in which the component materials and their relative geometry are emphasized. Descriptions of the components in detail follows.

The cell-block assembly. The cell-block, A in Figure 3, consists of a cylindrical molybdenum block 1.375-in. high and 1.21-in. outside diameter, with a concentric cylindrical cavity 1-in. in diameter and 0.875-in. deep. Three 0.125-in. diameter molybdenum rods screw into tapped holes in the bottom of the cell-block. Steel set screws hold the rods tightly in holes of the steel "crow's foot" C. The "crow's foot" is mounted on a ceramic ring D, which has an outside diameter of 4-in., an inside diameter of 3.5-in., and is 0.25-in. thick. Special ceramic spacers E, 1.0-in. in height and about 0.275-in. in diameter, connect the ceramic ring to



Relay 2 (Dawson)



Relay 2 (Modified)

Figure 1. Relay Modification

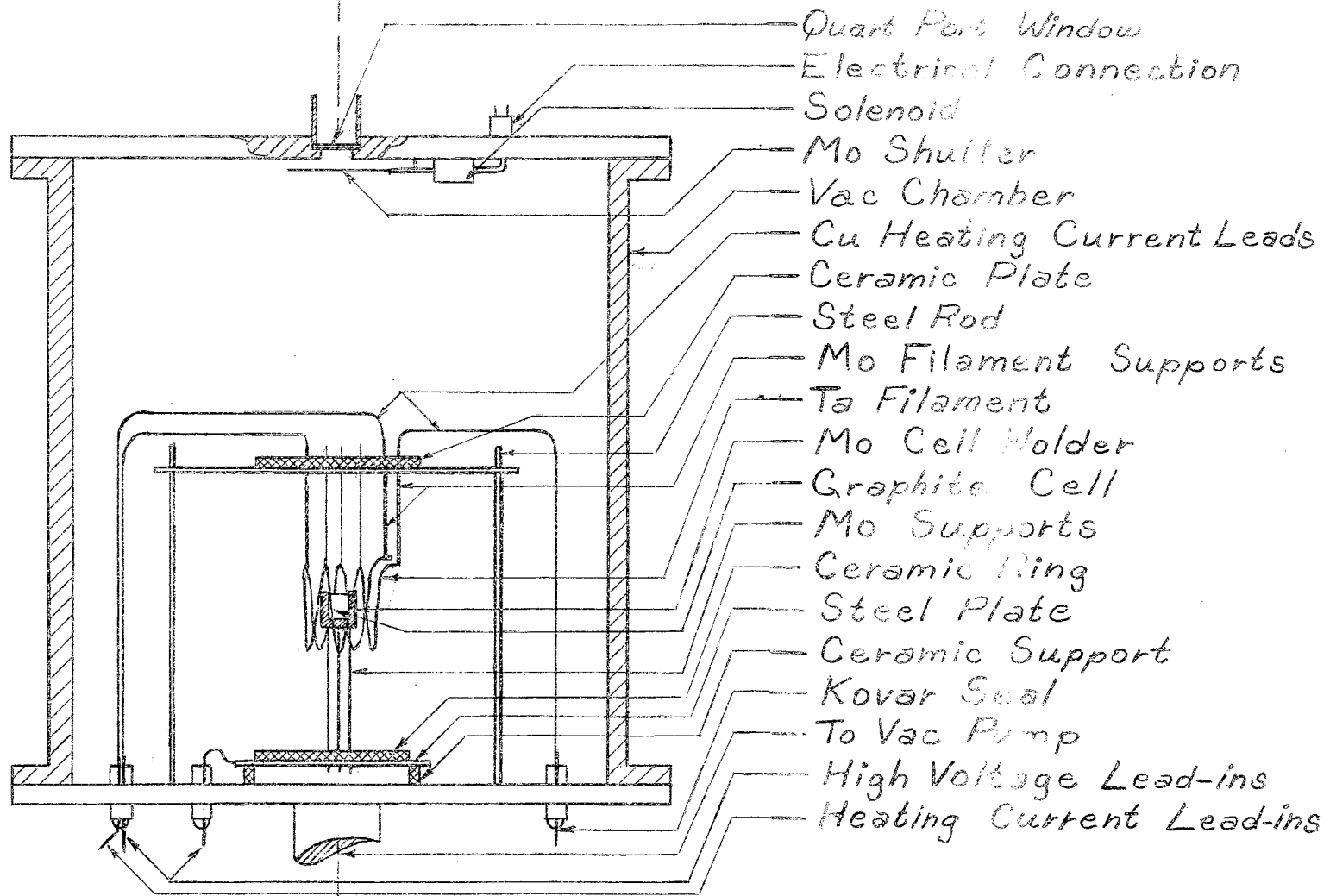


Figure 2. Electron Bombardment Furnace

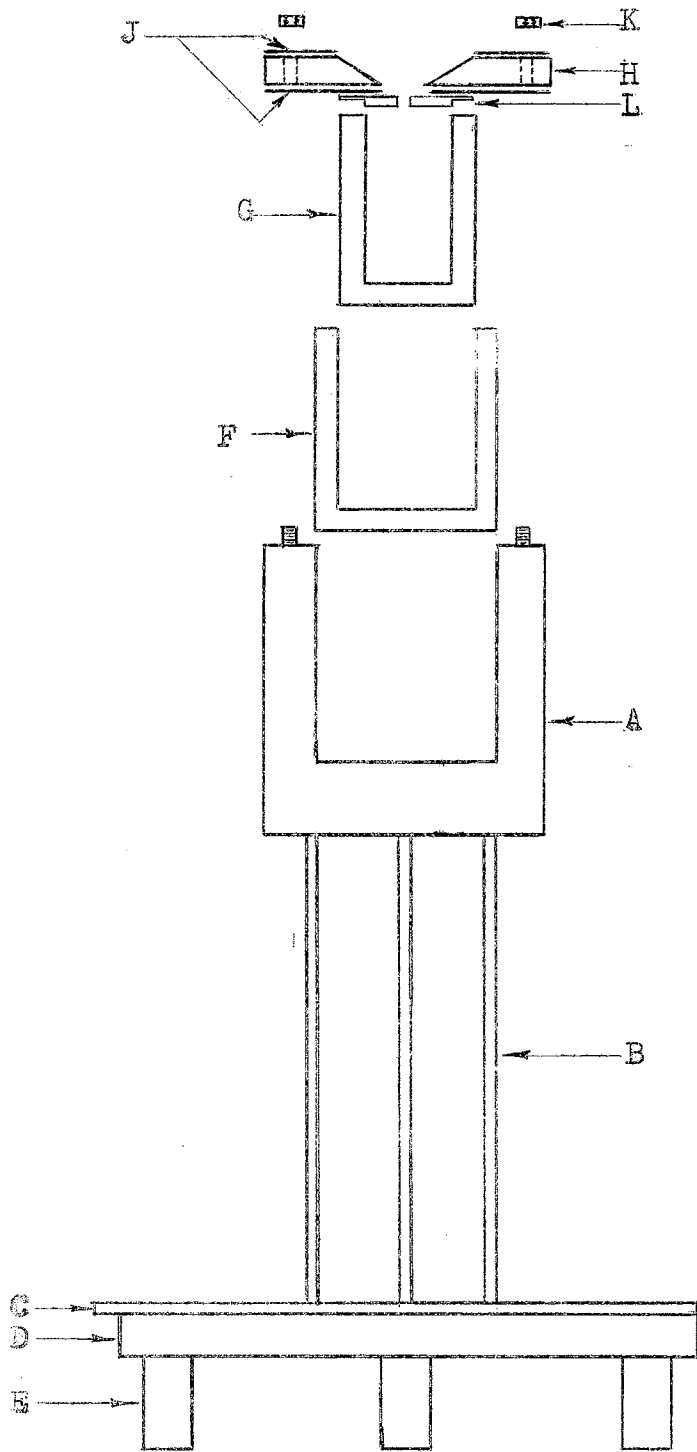


Figure 3. The Cell-block Assembly

the base plate. Radiation shielding (not shown in Figure 3) protects the base plate from the high temperatures of the cell-block region.

A cylindrical graphite shell F lines the cavity of the cell-block, and the graphite Knudsen cell G, which contains the sample, is located within the graphite liner. A thin graphite disc H, covered with 0.003-inch thick molybdenum J, serves as the top of the cell-block and is held in place by molybdenum nuts K. Lid H is not the lid of the Knudsen cell, which is represented by L -- rather its purpose is to eliminate as much as possible the uneven heating which occurs because of the opening in the top of the cell-block. The lid H has in its center a tapered hole of sufficient diameter to preclude interaction with the lid of species effusing from the Knudsen cell.

The Knudsen Cell. Knudsen cells of the same type described by Heydman (12) were employed for all vapor pressure measurements. Only graphite cells were employed. Initially it was assumed that gold and graphite are mutually inert at temperatures of interest to this work. However, it has been established that this is not true. Observations regarding the effect of the interaction of gold and graphite on the vapor pressure of gold are discussed within the experimental section.

Dimensions and constants for all Knudsen cells used in this work appear in Table I, in which D is the cell orifice diameter; A, the cross-sectional area of the channel hole;

TABLE I

KNUDSEN CELL CONSTANTS

<u>Cell</u>	<u>D (cm)</u>	<u>L/D</u>	<u>A (cm²x10⁻²)</u>	<u>W</u>
1	0.101	1.711	0.801	0.391
2	0.157	0.710	4.496	0.594
3	0.259	0.445	5.271	0.716
4	0.101	1.161	0.802	0.480
5	0.051	2.445	0.206	0.313
6	0.233	0.470	4.280	0.685

L , the length of the channel hole; and W , the Clausing Factor which is discussed in the section on calculations.

The filament. The filament is formed from a 100-cm. length of 0.030-in. diameter tantalum wire. It is sinusoidal in shape and supported so as to enclose the cell-block cylindrically. A typical filament is 6-cm. high and 5-cm. in diameter. These dimensions are not critical; they result from the size of the cell-block, i.e., the filament must be separated from the cell-block sufficiently to prevent arcing, and should extend above and below the cell-block far enough to assure uniform heating. The filament is supported at each bend by either 0.050-in. diameter tungsten or 0.060-in. diameter molybdenum wire. The two ends of the filament are connected to 0.125-in. diameter molybdenum rods which serve as supports and as current leads.

All filament supports are suspended from a ceramic ring of special design, which was fabricated by the McDanel Refractory Porcelain Co., Beaver Falls, Pennsylvania. This crucial component of the furnace is shown, with the method of securing the supports, in Figure 4.

The system of supports described above forms essentially a rigid structure, and the replacement of one filament by another of the same dimensions is accomplished by simply "threading" the wire over the supports. The ductility of 0.030-in. diameter tantalum wire makes this threading possible; such technique is not successful with tungsten wire.

In order to approximate the length of a given size of

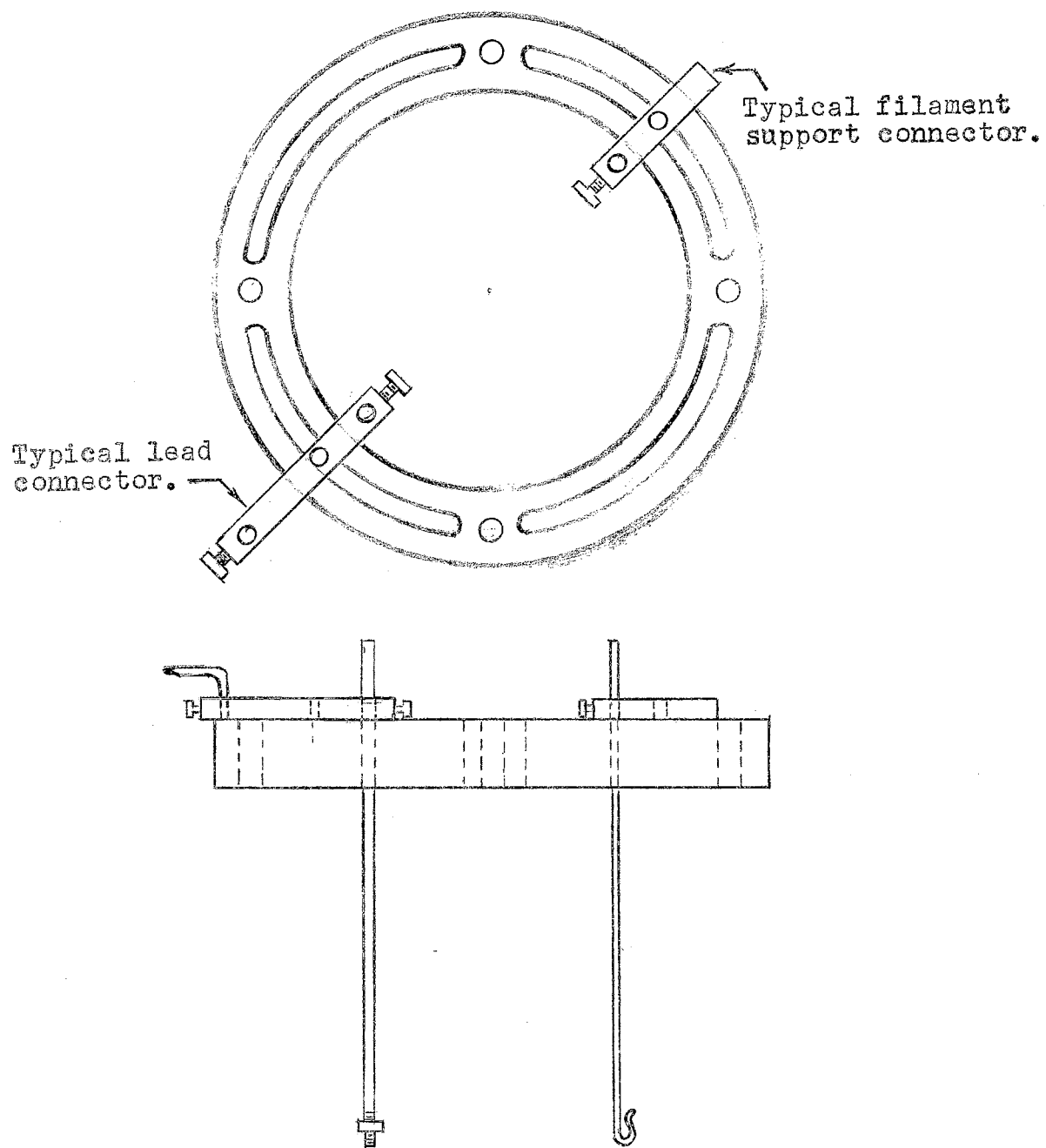


Figure 4. Ceramic ring with insulated connections.

wire which would provide the proper characteristics as a filament, the Dushman equation (5) was employed,

$$J = AT^2e^{-\phi/kT},$$

in which J is the saturation current density at the filament surface, A is a constant characteristic of the metal, k is the Boltzmann constant, and ϕ is the work function of the filament metal. Since J has dimensions of current per unit area, and since the maximum emission current in our case is fixed by the power supply design (see page 3), a knowledge of the work function ϕ and the constant A , both unique for a given metal at a specified temperature, allows calculation of the length of wire (of given cross-sectional area), which is necessary to supply 1.0 amp emission current at a given temperature. Calculations were made only as approximations, but they were found to be accurate within ± 10 per cent. The data required for the above mentioned calculations were obtained from the literature (11)(14)(17).

Radiation Shielding. Figure 5 shows the arrangement of the radiation shielding about the cell-block. All shielding components were fabricated from 0.003-in. molybdenum sheet. Three cylinders A, B, C are grouped concentrically about the cell-block; these cylinders are supported by three circular shields D which, with the circular shields G, complete the shielding at the bottom of the furnace. The shields G are attached directly to the cell-block supports by notching the supports and twisting molybdenum wire to form a pin at each notch. The shields G are thus at the same potential as the

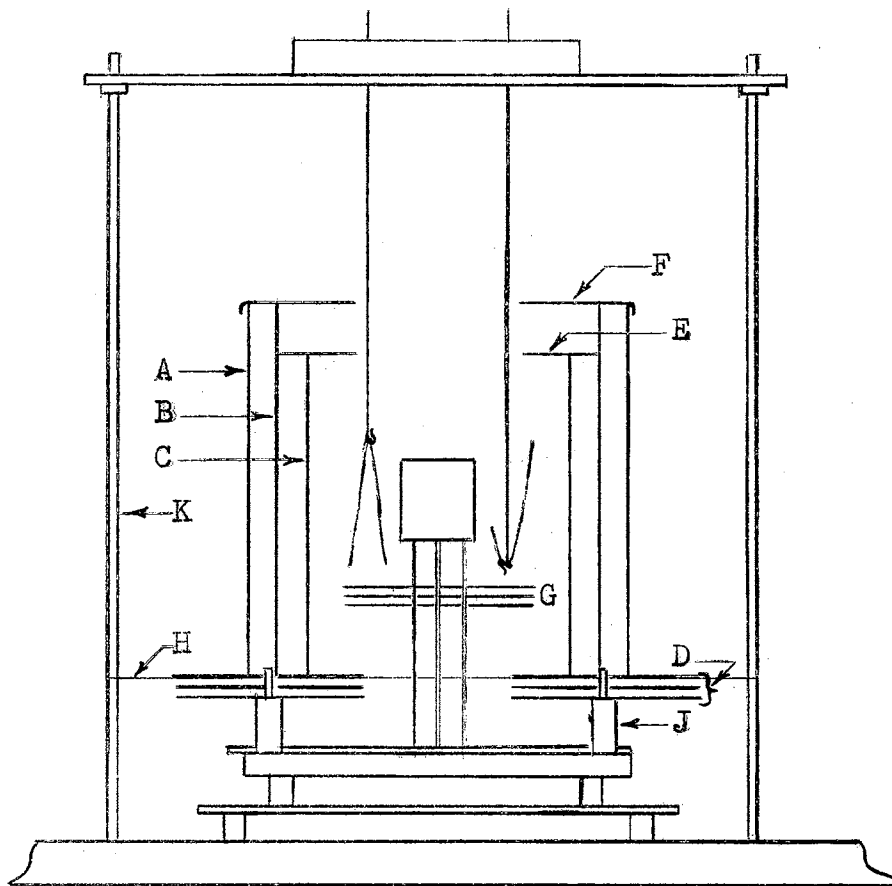


Figure 5. The Radiation Shielding Arrangement.

cell-block and must be insulated accordingly. The shields D are supported by ceramic spacers J and by a 0.015-in. diameter molybdenum wire stretched tautly about the steel rods K. The result of this arrangement is, at the bottom and the sides, a closed container as far as the radiation emitted from the cell-block is concerned, i.e., no radiation escapes by traveling in a straight line from the cell-block. The situation is not as satisfactory at the top. Here, much less shielding E, F is feasible because of the space required for the filament supports. The result is a rather large aperture, slightly larger than the diameter of the filament, through which radiation can escape directly from the cell-block. This is not a desirable feature, but it is inherent with the type of filament described.

The electrical leads. All electrical leads to the filament and cell-block enter the vacuum chamber through the bottom. The type of coupling described by Heydman (12) was employed; the lead-in is attached by a Kovar Seal to a 29/42 standard tapered joint. American Standard Gage no. 5 stranded copper wire (7 strands) completes the filament current circuit within the vacuum chamber --- American Standard Gage no. 10 copper wire, the high voltage circuit. The two filament current leads, and one of the high voltage leads, terminate at molybdenum mounts on the upper ceramic ring, as in Figure 4. The other high voltage lead is fastened by a set screw to the steel "crow's foot" which is connected to the cell-block via the cell-block supports. No serious dif-

difficulty was encountered in the use of copper wire to make these connections, though the wires did become hot enough to make soft solder unsuitable for the connections at the Kovar lead-ins; these connections were made with silver solder. A minor difficulty was the loosening of set screws due to repeated thermal expansion and contraction.

The observation port and the shutter mechanism. The observation port, which is directly above the cell-block, is described by Heydman (12). Initially, Pyrex port windows were employed, but after several of these cracked while the furnace was in operation (presumably from thermal shock), they were replaced by quartz windows 0.25-in. thick and 2-in. in diameter. No further difficulties were encountered.

A 2.5-in. diameter by 0.003-in. thick molybdenum shutter, operated by a solenoid, protects the port window from thermal radiation and the excessive accumulation of condensate. The solenoid is mounted in close thermal contact with the underside of the vacuum chamber lid, which is cooled by water circulating through 0.25-in. copper tubing soldered onto the outside of the lid. The shutter is attached to a molybdenum rod, 6-in. long and 0.125-in. in diameter, which is fixed to the underside of the lid by a pivot 3-in. from the center of the shutter. The solenoid arm is connected to the pivot at right angles to the shutter arm. A steel spring returns the shutter to the closed position when the solenoid is de-activated.

Electrical leads to the solenoid enter the vacuum sys-

tem through a ceramic connector soldered into the top of the lid. An electrical socket, mounted on the outside of the lid, allows the connection to be broken when the lid is removed.

The vacuum system. A detailed description of the vacuum system employed in this work is given by Heydman (12), and only the essential features will be mentioned here.

The vacuum chamber consists of a section of cold-rolled steel pipe, 12-in. inside diameter and 12-in. long, with 0.75-in. thick steel flanges welded on the top and bottom. The top flange has O-ring grooves; the bottom flange is flat and seats on O-rings in the base plate of the chamber. The valve arrangement allows the vacuum chamber to be isolated from the rest of the vacuum system; thus the vacuum chamber can be opened to the atmosphere without shutting off the diffusion pump.

The steel vacuum lines described by Heydman were replaced by 1.5-in. inside diameter copper tubing. To minimize vibrations, which shortened the useful life of the tungsten filaments initially used in the furnace, the mechanical pump was bolted through rubber stoppers to the concrete floor, and a flexible brass bellows was installed between the mechanical pump and the remainder of the vacuum system.

The one other modification of Heydman's system was the installation of a thermistor in the vacuum line, with necessary connections to permit its use as a leak detector. The leak detector circuit, constructed in this laboratory, will

be described by J. G. Edwards in his Ph. D. thesis.

The lowest pressure observed for this system was less than 1×10^{-6} Torr; operating pressures of less than 3×10^{-5} Torr were easily maintained for temperatures up to about 1800°C . The system would pump down from atmospheric pressure to $2\text{-}3 \times 10^{-6}$ Torr in about three hours. Pressures down to about 1×10^{-2} Torr were measured with a Hastings Gage, type 6V-3RS; a Phillips Discharge Gage, type PHG-27, was used to measure pressures from 1×10^{-2} to 1×10^{-6} Torr. The Phillips gage was adjusted to agree with a Veeco heated cathode gage, type RG-2A.

Discussion. Perhaps the most obvious choice for the geometry of a filament for the furnace described above is the helix. Helical filaments, made initially from 0.030-in. diameter tungsten wire and later from 0.030-in. and 0.040-in. diameter tantalum wire, were the first type employed. The ease of fabrication and the assurance of a high degree of symmetry make such filaments attractive for use. They have the serious shortcoming, however, of being extremely susceptible to distortion at high temperatures. Distortion of the filament can result in uneven heating of the cell-block and can reduce (or even close) the gap between the filament and the cell-block, which are normally separated by vacuum. Several times, distortion of helical filaments occurred to such an extent that an electrical short resulted between the filament and the cell-block.

Thermal distortion, a mechanical property of the fil-

ament material, would be expected to depend largely on the diameter of the helix. Rocco and Sears (19) successfully used a helical filament of 0.020-in. diameter tungsten wire. Their filament had five turns, but the diameter of the helix was only 0.25-in. They reported no difficulty due to distortion. Such a relatively small filament is impractical for the furnace described here. Efforts were made to support the necessarily large filament. But the procedure of adding more and more support to the filament did not prevent distortion completely; furthermore, the cold spots produced at the points of support are as undesirable as the distortion itself.

Sinusoidal filaments of tungsten tend to distort in spite of seemingly adequate support, though this tendency is not as marked as in the case of the helix. The brittleness of once-heated tungsten wire precludes the reshaping of a distorted filament; hence, supporting the filament as much as is practical, and then accepting the distortion which occurs, works best. This is similar to the technique of Chupka (2) and others, who use a filament consisting of two loops in series, made from a single piece of wire. The filament is supported in place and allowed to distort, uniform heating being assured by the interposition of a cylindrical target between the filament and the cell.

Initially, the cell-block was suspended from a ceramic ring, as shown in Figure 6a. The filament was located as shown with respect to the top of the cell-block. Several

vapor pressure determinations on gold were made with this geometry; these measurements showed inconsistencies well outside the experimental error of the method. Examination of the Knudsen cell revealed that gold had condensed in the cell orifice; this clearly indicated a temperature gradient with a cold spot in the vicinity of the cell orifice. The elimination of this temperature gradient involved three considerations, all suggested in Figure 6a: (1) The top of the cell-block is primarily graphite, while the sides and bottom are of molybdenum. The difference in the emissivity of graphite and molybdenum and the thinness of the lid compared to the sides and bottom could result in a relatively cold top. (2) Support of the filament occurs at points which are roughly in the same plane as the orifice, and cold spots occur at points of support due to heat loss by conduction. Cold spots result in lowered emission current from the affected segments of the filament. (3) The supports of the cell-block, located at the top, could easily receive an inordinate portion of the bombardment current, thus partially shielding the lid of the cell-block.

Modifications resulting from the above considerations appear in Figure 6b. Here, the filament supports are considerably above the plane of the cell orifice, the cell-block is supported from the bottom, and 0.003-in. thick molybdenum sheet has been added to the top of the graphite cell-block lid. Later, it was found that the extra bends in the filament are unnecessary, if the filament extends far

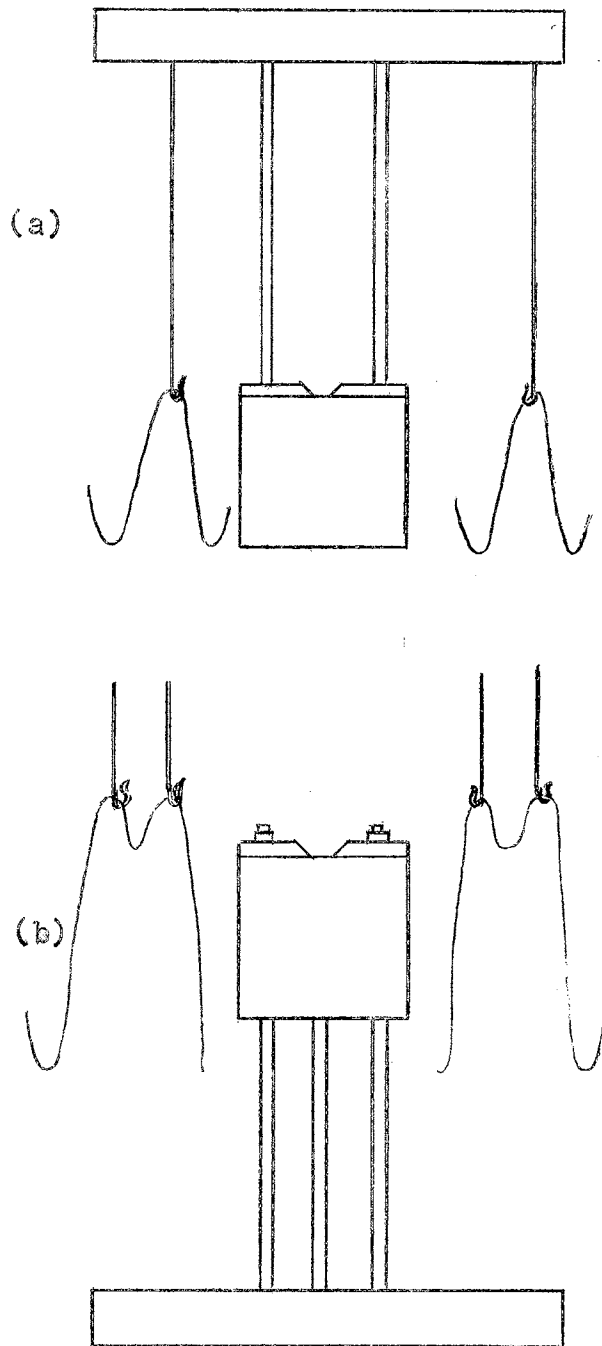


Figure 6. Cell-block Geometries.

enough above the cell-block to remove the cold spots at points of support from the plane of the cell orifice. These changes eliminated the temperature gradient, at least to the extent that no subsequent condensation of gold in the cell orifice was detected.

The availability of component materials and the convenience of fabrication largely determined the dimensions of the furnace described above. The author feels that reduction of the furnace dimensions by a factor of two or three would constitute a definite improvement of the system. With a smaller system, the aperture in the radiation shielding could be greatly reduced. Also, the problem of filament distortion would decrease; accordingly, less filament support would be required, and uniform heating of the smaller cell-block would be enhanced. A minor advantage of the suggested smaller system would be the decrease in time required for evacuation.

Auxiliary Apparatus.

Temperature measurement. All temperature measurements were performed with a Leeds and Northrup Model 8622-C optical pyrometer, serial number 1313042, which was calibrated by comparison with one of the same type which has been calibrated by the National Bureau of Standards. Temperatures measured with the working pyrometer required no corrections, agreement with the N. B. S. calibrated instrument being within the smallest scale division (5° on the H scale and 10° on the xH scale).

Weight measurements. Weight losses were determined to the nearest 0.01mg by weighing the Knudsen cell before and after each run on a Sartorius-Werke semi-micro balance, Model SM 10/100 g.

Time measurements. Time measurements were made with a Running Time Meter, type 640E, manufactured by the Cramer Controls Corporation. The timer, incorporated into the power supply control panel, measures time in one second counts.

Measurements and observations via microscope. A traveling microscope, manufactured by David W. Mann Precision Instruments, serial number 28327, was very valuable in this work. Diameters of the Knudsen cell orifices were determined to the nearest 0.0001-in. with the instrument. The microscope was also used to inspect the cell orifices for gold condensation and to examine the gold samples for graphite contamination.

PART III
EXPERIMENTAL

Performance of the Furnace.

The best procedure for operating the furnace was found to be the following:

1. The vacuum chamber was evacuated to less than 1×10^{-5} Torr.

2. Filament current was increased slowly until the filament became hot enough for thermionic emission.

3. Potential was applied between the filament and the cell-block. After some experience, the temperature of the cell-block and the rate of temperature increase could be estimated from the control settings and the rate of increase of the bombardment current. Consequently, the approach to the desired temperature could be made on the basis of control panel observations alone, finer adjustments being governed by optical pyrometer sightings.

4. Once the desired temperature was attained, the servo mechanism for controlling the bombardment current was energized.

From this point on, the temperature should not vary more than 2 or 3 degrees. However, in many of even the most well-behaved runs, subsequent adjustments of the control settings were necessary. This was usually because of a

drifting increase in the temperature of the cell-block, thought to be due to the large heat capacity of the cell-block and its surroundings. Thermal feedback from the cell-block to the filament compounds the problem: A slow approach of the cell-block temperature to equilibrium because of large heat capacity produces a gradual increase in emission current, which causes a further increase in cell-block temperature, etc.

Heating curves. Some typical time vs. temperature plots appear in Figure 7. From the curves shown, it is apparent that for a well-behaved run the temperature remains constant within the accuracy of the optical pyrometer. The irregular heating curves for some of the runs shown are due to adjustment, while heating, of the power supply in order to attain a desired temperature. It is also apparent that the time required to reach run temperature and the cooling time are generally much less than the time of the run.

Discussion. The measure of success of a furnace designed for vapor pressure studies is the degree to which it will maintain a desired temperature for a necessary time. The temperature control for this system is based on the assumption that a constant bombardment current will result in a constant temperature. Fluctuations in the bombardment current are counteracted as described by Dawson (4); however, there are several factors which should be mentioned in a qualifying sense. In this system a control signal, obtained by passing the bombardment current through a precision re-

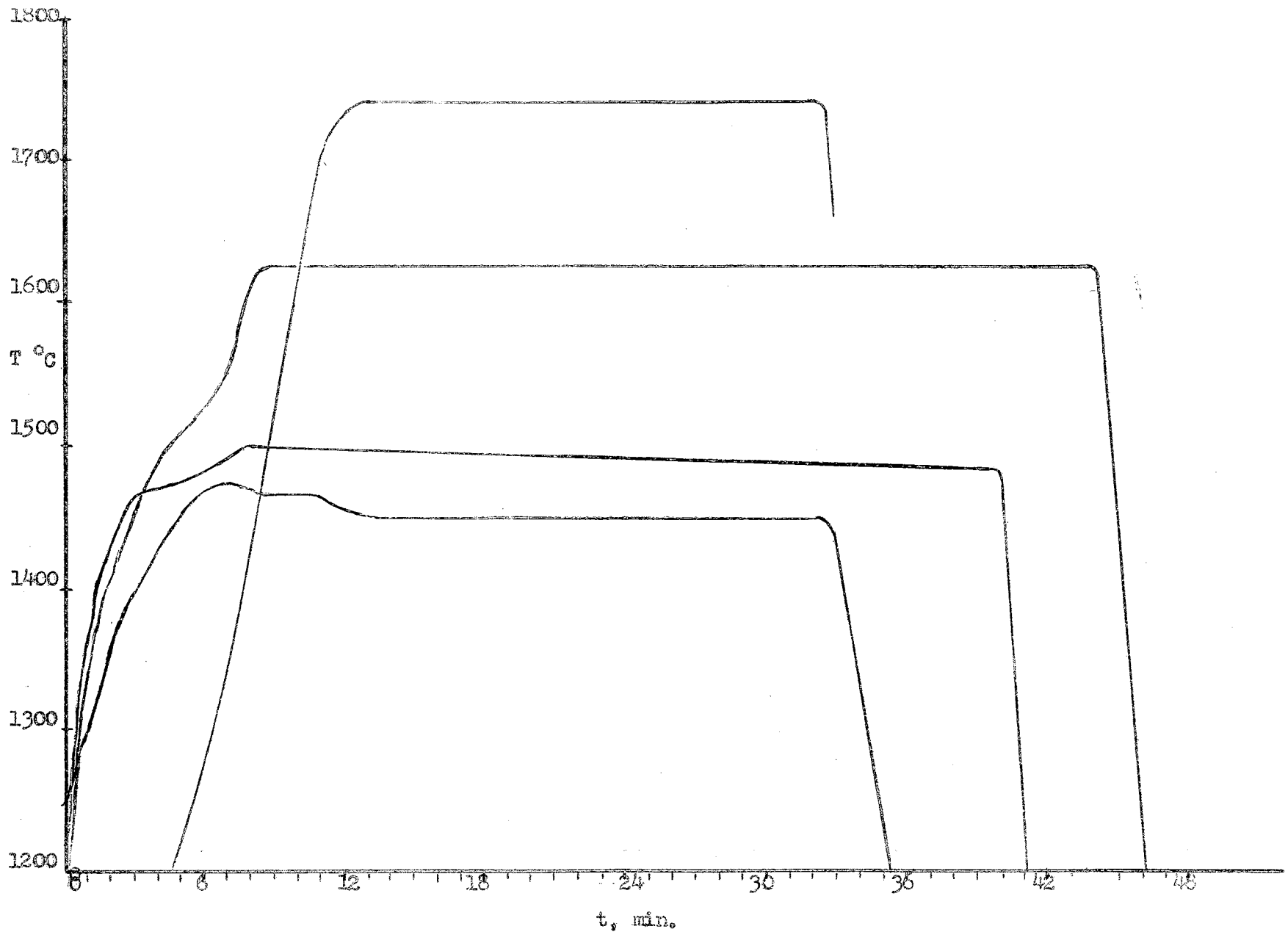


Figure 7. Typical Heating Curves

sistor, is fed into a servo-amplifier. The output of the amplifier operates a servo-motor so as to counteract bombardment current fluctuations, i.e., a control value for the bombardment current is preset, and the servo-motor reduces the filament heating current if the bombardment current exceeds the control value, and vice versa.

The extreme sensitivity of the bombardment current to very small changes in the filament temperature presents the most serious difficulty to the above method of temperature control. The effects of this sensitivity appear in Table II, in which the heating current I supplied to the filament is a measure of the filament temperature, B is the bombardment current, and V is the potential between the filament and the cell-block. For the data in Table II, the cell-block temperature varied from about 1000°C to above 1800°C . Thus a change of 2 amp in this case has increased the bombardment current by about 900 ma, causing the cell-block temperature to increase more than 800° . Difficulty in controlling these variables manually has contributed, probably more than any other factor, to the relative obscurity of electron bombardment heating for vapor pressure studies.

The main difficulty actually experienced with the temperature control resulted from a tendency of the servo-motor to oscillate when subjected to bombardment current fluctuations of greater than about 20 ma. Oscillations, once begun, occurred across the control value of the bombardment current; left unchecked, the output of the Variac operated by the servo-motor would oscillate between zero and the full 115 volts.

TABLE II

TYPICAL CONTROL VALUES

<u>I (amp)</u>	<u>B (ma)</u>	<u>V (dc)</u>	<u>T °C</u>
20	120	3000	1000
21	240	3000	
22	>1000	2750	>1800

between the effusing species and the surface of the channel hole through which they effuse, for any hole of finite length. The theoretical evaluation of \underline{W} is based primarily on the work of Clausing (2). However, the reader is referred to the work of Freeman (6) for information concerning "the veritable mélange of theories, equations, correction factors, etc., pertinent to measurement of vapor pressures by the effusion methods." For this work, values for \underline{W} were obtained by interpolation of those given by Heydman (12), who has tabulated \underline{W} values in terms of L/D , the ratio of the length of the channel hole to its diameter.

End corrections. If any information is available regarding the vapor pressure of the substance being studied, a correction is possible for the time involved in heating the Knudsen cell to the temperature and cooling it from the temperature of the run. One way to set up this correction is in terms of the weight loss as follows.

Let \underline{T}' be the weighted average of the temperatures observed while heating for \underline{t}' seconds to the actual run temperature, \underline{T} . The corresponding Knudsen equation is

$$p' = \frac{g'}{WAt'} \left(\frac{2RT'}{M} \right)^{1/2}$$

Now assuming a value for the vapor pressure P at \underline{T} , the equation

$$P = \frac{g}{WAt} \left(\frac{2RT}{M} \right)^{1/2}$$

can be written. Solving these two equations for g' and g respectively, and equating the results gives the time \underline{t} ne-

cessary to effuse g' at T instead of at T' :

$$g' = WAt'P' \left(\frac{M}{2RT'} \right)^{1/2} = g = WAtP \left(\frac{M}{2RT} \right)^{1/2}$$

or $\frac{t'P'}{(T')^{1/2}} = \frac{tP}{(T)^{1/2}}$, which gives $t = \frac{t'P'}{P} \left(\frac{T}{T'} \right)^{1/2}$. Corrections

for cooling are analogous. Typical corrections amount to about 3% of the total run time.

Temperature corrections. Temperature measurements required correction because of the condensation of effusing gold on the quartz window; this correction was determined by viewing a tungsten filament lamp with the optical pyrometer — first through the coated quartz window, and then with the window absent. The difference between the two temperatures obtained in this manner is the correction for the deposit on the quartz window and the window itself.

Results.

Vapor pressure data for gold from this work appear in Table III. These data, and those obtained by Heydman, are presented in Figure 8 in the customary log P vs. $1/T$ plot. The numbers within the cell symbols denote the chronological order of the runs.

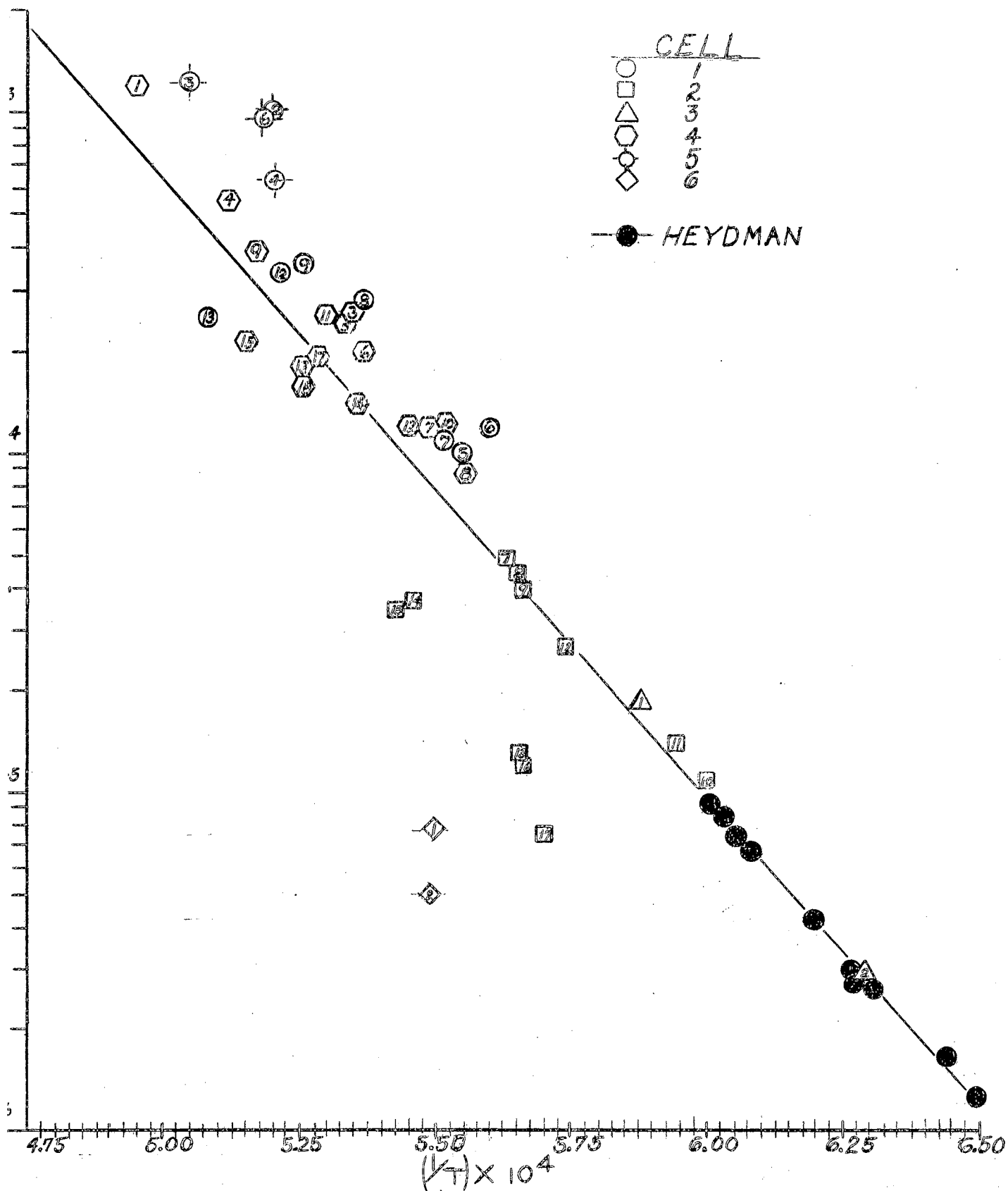
Discussion. Initially, it was assumed that gold and graphite are mutually inert, and that graphite should be a suitable material from which to construct the Knudsen cells for containing the gold sample at high temperatures. Hansen (8) reports negligible interaction between gold and graphite at temperatures up to the boiling point of gold. Hansen quotes from the work of Moissan (18): "At its boiling point

TABLE III
VAPOR PRESSURE OF GOLD

<u>T °K</u>	<u>Cell</u>	<u>t, sec</u>	<u>g, mg.</u>	<u>P, atm x 10⁵</u>
1783	1	3730	20.73	12.
1793	1	2930	13.38	10.
1810	1	1690	8.28	11.
1858	1	1313	16.50	28.
1900	1	1900	29.89	36.
1917	1	1898	27.65	34.
1968	1	1810	19.18	1.1
1663	2	3947	17.14	1.4
1683	2	3715	20.06	2.7
1742	2	1280	13.56	0.76
1748	2	3120	9.29	4.3
1763	2	1830	32.49	3.9
1763	2	2185	33.14	1.3
1763	2	2410	12.06	1.2
1766	2	2620	12.07	4.7
1768	2	1948	35.42	3.6
1831	2	1850	25.40	2.5
1838	2	1570	15.12	0.29
1593	3	2050	2.39	1.9
1698	3	2048	22.04	8.9
1800	4	3765	18.90	11.
1811	4	4850	29.15	12.
1817	4	2505	17.47	12.
1833	4	2790	18.95	20.

TABLE III (CONTINUED)

<u>T °K</u>	<u>Cell</u>	<u>t, sec</u>	<u>g, mg.</u>	<u>P, atm x 10⁵</u>
1859	4	2265	27.52	20.
1863	4	1905	14.44	14.
1873	4	1605	23.24	26.
1890	4	2210	30.91	25.
1893	4	2220	29.64	24.
1893	4	1350	14.07	19.
1898	4	2200	21.26	18.
1900	4	1650	14.20	16.
1936	4	2100	44.40	39.
1943	4	2000	23.12	21.
1955	4	1795	53.80	55.
2016	4	1510	101.33	120.
1918	5	1800	10.44	64.
1923	5	2260	20.45	100.
1931	5	2490	21.80	97.
1978	5	1665	18.46	124.
1816	6	2210	10.64	0.77
1820	6	3715	9.36	0.40



(approximately 2970°C), gold dissolves carbon, which crystallizes on cooling in the form of graphite."; the work of Hempel (10), where the solubility is reported as about 0.3% by wt.; and that of Ruff (20), in which the solubility is given as "traces or unweighably small amounts." However, the results of this work show that graphite is only conditionally suitable as a container material for gold; the suitability of graphite for this purpose depends simply on the total time of heating.

After prolonged heating, the interaction between gold and graphite produces a drastic reduction in the rate of weight loss of gold from the Knudsen cell, and once this effect appears, it becomes increasingly worse with subsequent heatings. The behavior of cell 2 in Figure 8 shows this effect of graphite contamination on the measured vapor pressure of gold. Cell 2 is one of the cells which was also used by Heydman. It is estimated that this cell was heated for at least 14.5 hrs. at an average temperature of 1700°K up to run 13. After run 13, visual examination showed the gold sample from the cell to be coated with a graphite layer. Runs 14, 15, 16, 17 were each followed by examination of the sample under a microscope; the graphite coating increased with each run.

The sample from cell 2 was then placed in cell 6 (a new cell) and runs 1 and 2 were made with this cell, after which the graphite coating on the sample completely obscured the gold. The vapor pressure calculated for run 2, cell 6, is

low by a factor of twenty.

In order to check the time dependence of the effect mentioned above, runs were made with cell 4 until the total time of heating was approximately 7.4 hrs. at an average temperature of 1880°K , i.e., runs 1 through 11. After run 11, the cell was heated for 3 hrs. at $1948\text{-}1973^{\circ}\text{K}$; run 12 was then made. After run 12, the cell was again heated for about 3 hrs. at $1948\text{-}1973^{\circ}\text{K}$. Examination of the sample through a microscope after each heating showed the graphite contamination to be increasing. After run 12, the total time of heating for cell 4 was about 13.4 hrs., which corresponds approximately to the state of cell 2 after run 12. Runs 13, 14, 15, 17, 18 for cell 4 show the same general behavior as the corresponding runs for cell 2, although the average temperature at which cell 4 was heated is considerably higher than that for cell 2. Thus, the time required for the interaction to become appreciable apparently is not determined by the cell temperature, although the extent of interaction, as measured by depression of the vapor pressure apparently does depend on temperature.

Examination of the sample from cell 5, run 2, gave information on the early stages of the growth of the graphite coating on the gold sample. After run 2 the graphite was only faintly visible on the gold surface. The gold in the Knudsen cell, on cooling, solidifies into a nugget with a flat bottom and a vertical cross-sectional profile which is convex upward. Examination of this nugget under a micro-

scope revealed very beautiful patterns on the curved surface. The flat underside of the nugget, on which no graphite was visible, showed no such formations but appeared as a bed of small spheres (typical diameter of about 0.0028-in.). Sketches from microscopic examinations appear in Figure 10. The basic feature of these patterns is an orthogonal orientation. These patterns became less pronounced after run 3, cell 5, while the graphite coating increased in thickness. After run 4, cell 5, the patterns were obscured completely, and the underside of the nugget was also covered with graphite.

The appearance of the patterns on the surface of the nugget suggests a change of phase, and if they are due to graphite, this would be interpreted as the crystallization of dissolved carbon from the molten gold on cooling.

With a copper x-ray source, a 114.59 mm diameter Philips Debye Scherrer Type No. 52056-B Powder Camera, and a nickel filter, x-ray diffraction patterns were obtained for the following samples:

1. Gold, 99.95% plus.
2. Pure graphite from the stock which was used to construct the Knudsen cells.
3. A scraping from the surface of a graphite-contaminated nugget.
4. A filing from the interior of a graphite-contaminated nugget.

The diffraction pattern results bring out the following

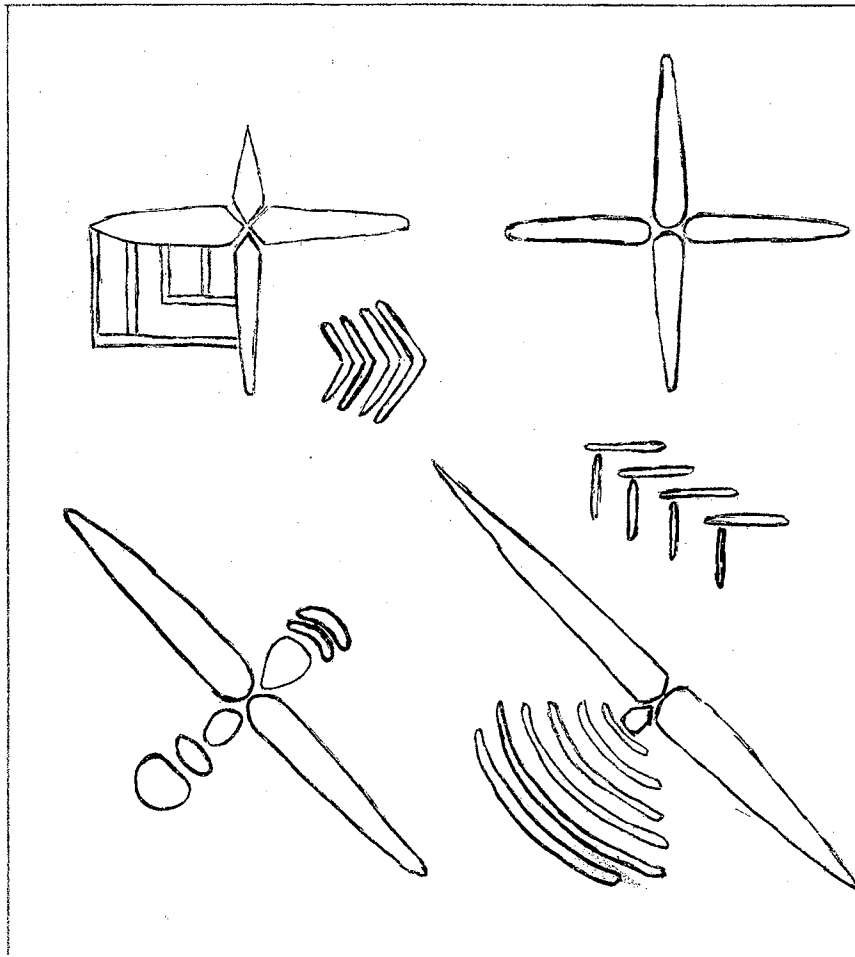


Figure 9. Sketch of Patterns Observed on the surface of Gold Sample.

facts:

1. The lines due to gold in the sample from the surface of the nugget are the same as those for pure gold.

2. The lines due presumably to graphite in sample 3 above are not the same as those of pure graphite of sample 2. Efforts to find known diffraction patterns of graphite with which to compare these lines were unsuccessful.

3. The sample from the interior of the nugget revealed only three very faint lines other than those lines attributable to pure gold. These three lines also appear on the pattern from the surface of the nugget.

D-values from the Bragg equation (1) are tabulated in Table IV, with details of the powder diffraction patterns. From these data, and from the observations of the preceding discussion, the primary interaction between gold and graphite appears to be a surface phenomenon. However, this conclusion is reached solely by examination of the sample after solidification, and does not necessarily apply to the molten state. For example, the "freezing-out" of dissolved carbon on cooling the sample would be expected to give rise to the same data which are presented here, but whether this is actually the case is indeterminable from these data. A study of the Au-C system in the molten state is needed to describe the full extent of the interaction reported here.

Figure 10 shows the vapor pressure data for gold which were obtained before the contamination effect appeared; the data of Heydman (12) are included. These combined data es-

TABLE IV
X-RAY DIFFRACTION DATA

Interior of Nugget
(6 hrs., 35KV, 20ma)

<u>Line No.*</u>	<u>d</u>	<u>Intensity</u>
1	4.1486	1
2	3.7354	3
3	1.9877	2

Surface of Nugget
(6 hrs., 35KV, 20ma)

<u>Line No.*</u>	<u>d</u>	<u>Intensity</u>
1	4.1678	1
2	3.7509	3
3	2.8289	v.w.
4	1.9959	2
5	1.7354	v.w.
6	1.5813	v.v.w.

Graphite Used in Knudsen Cell
(6 1/2 hrs., 35KV, 20ma)

<u>Line No.</u>	<u>d</u>	<u>Intensity</u>
1	3.3482	4
2	2.8115	v.w.
3	2.4402	v.w.
4	2.3247	v.w.
5	2.1016	1
6	1.9918	5
7	1.8294	2
8	1.7384	6
9	1.4847	v.w.
10	1.2858	2 1/2
11	1.1019	2 1/2
12	1.0627	3

*All lines attributable to pure gold omitted.

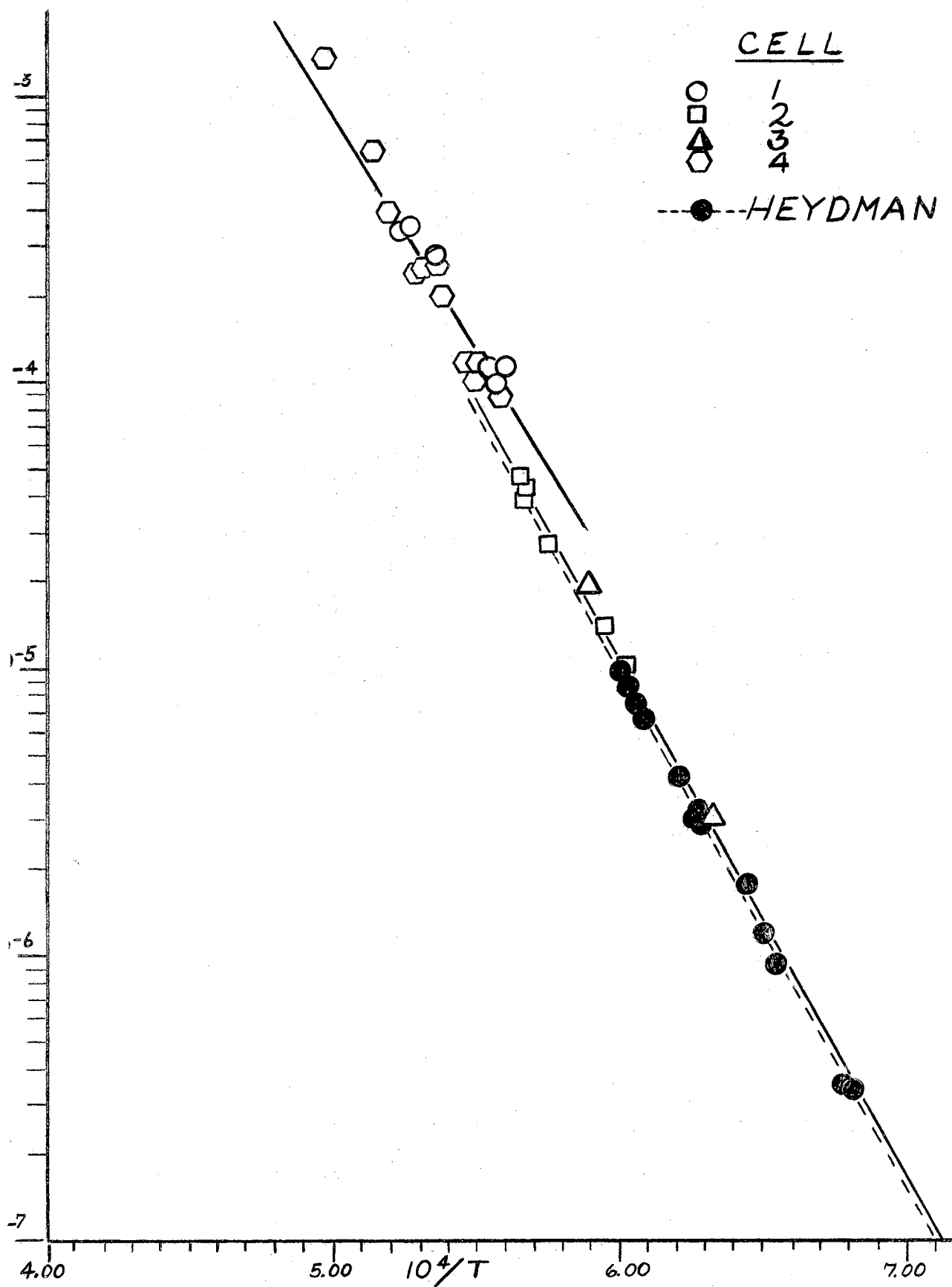


Figure 10. Vapor Pressure of Gold.

establish not the expected single straight line, but two lines: part of the data from this work agrees with the lower line established by Heydman, while the remainder of the data indicates a somewhat higher vapor pressure. The data from this work which comprise the lower vapor pressure curve yield a least squares equation of $\log P = 5.8810 - 18118/T$, which compares excellently with Heydman's least squares equation, $\log P = 5.9083 - 18224/T$. The data from this work which comprise the higher vapor pressure curve in Figure 10 yield a least squares equation of $\log P = 5.4453 - 17000/T$.

All of the data from this work which agree with the vapor pressure of Heydman were obtained by using the same Knudsen cells used by Heydman, while the data which comprise the upper curve of Figure 10 were obtained with new Knudsen cells. The apparent discrepancy in these data may be explained in terms of the difference in the orifice dimensions of the Knudsen cells, given in Table I.

In the derivation of the Knudsen equation, the assumption is made in effect that the equilibrium vapor pressure of a species in a closed container is not disturbed by the removal of a small cross-sectional area from the container wall to form an orifice. The accuracy of this assumption depends on the size of the cross-section removed. That this is true may be seen by considering that the equilibrium state depends on the rate of evaporation being equal to the rate of condensation. Any hole in the container decreases the rate of condensation; accordingly, the smaller the hole,

the smaller the displacement from equilibrium, and the more accurate the original assumption. Actually, the orifice size alone does not determine the shift from true equilibrium in the cell, rather the ratio of the orifice cross-sectional area to the effective vaporizing area of the sample. But in our case the Knudsen cells are the same size; hence, the area of the sample is the same for all cells, provided the molten sample covers the bottom of the cell. Thus it is correct to consider the shift in measured vapor pressure to be a function of only the orifice cross-section.

Conclusion. On the basis of the preceding discussion, the higher vapor pressure curve in Figure 10 gives the vapor pressure of gold more accurately than the lower curve. The four runs with cell 5, Figure 8, indicate that the vapor pressure of gold may be slightly higher than that given by the upper line of Figure 10; in any case, the upper line of Figure 10 establishes a lower limit for the vapor pressure of gold.

Figure 11 presents a graphical summary of vapor pressure data for gold available at the time of this work.

Heats of sublimation calculated from the experimental vapor pressure data appear in Table V. From these data, the best value for the heat of sublimation of gold at 298.15°K , obtained by averaging only those runs which establish the higher vapor pressure curve in Figure 10, is 86.67 Kcal per mole, with an average deviation of 0.50 Kcal. The free energy functions necessary for these calculations were taken

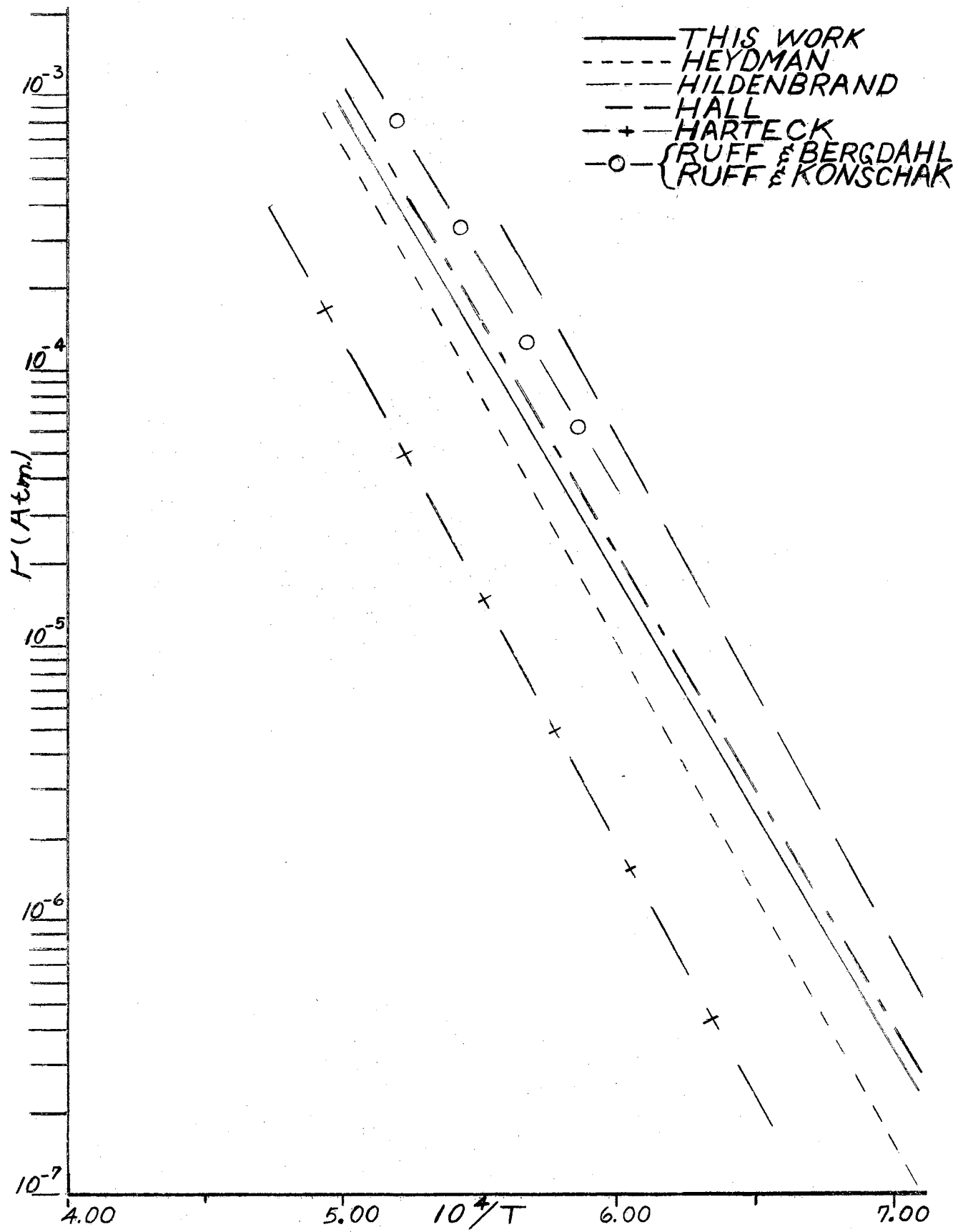


Figure 11. Graphical Summary of Available Information on the Vapor Pressure of Gold.

TABLE V

HEAT OF SUBLIMATION OF GOLD

T °K	$\Delta F^\circ/T$	$\Delta(F^\circ - H^\circ_{298})/T$ _g	$\Delta(F^\circ - H^\circ_{298})/T$ _l	$\Delta H^\circ_{298}/T$	ΔH°_{298}
1783	17.94	47.88	18.03	47.79	85.21
1793	18.31	47.90	18.07	48.14	86.32
1800	18.53	47.91	18.10	48.34	87.01
1810	18.11	47.94	18.14	47.91	86.72
1811	18.11	47.94	18.14	47.91	86.76
1817	17.94	47.95	18.16	47.73	86.72
1833	17.94	47.98	18.24	47.68	87.40
1858	16.26	48.05	18.34	47.95	85.41
1859	16.92	48.05	18.34	46.65	86.72
1873	16.40	48.08	18.39	46.09	86.33
1890	16.48	48.12	18.46	46.14	87.20
1893	16.56	48.13	18.48	46.20	87.46
1900	15.76	48.14	18.50	45.40	86.26
1917	15.87	48.18	18.57	45.48	87.18
1936	15.60	48.22	18.63	45.19	87.49
1955	14.92	48.26	18.71	44.47	86.94
2016	13.36	48.38	18.92	42.82	86.32

from Stull and Sinke (21). Table VI summarizes the various values for the heat of sublimation of gold at 298.15°K. The value from Kelley's compilation (15) is based on the vapor pressure data of Harteck (9), while that from Stulle and Sinke (21) is based on the work of Hall (7). Hildenbrand's value was calculated from Hildenbrand's vapor pressure data (13) by this author with the use of the third law technique and free energy functions from Stulle and Sinke (21).

TABLE VI

SUMMARY OF ΔH_{298}° FOR GOLD

<u>Source</u>	<u>ΔH_{298}° (Kcal per mole)</u>
Heydman (12)	88.4
Hildenbrand (13)	86.5
Kelly (15)	90.5
Stulle and Sinke (21)	84.7
This work	86.7

PART IV
BIBLIOGRAPHY

1. Bragg Equation, See Any Standard Physical Chemistry Text.
2. Chupka, W. A., Private Communication.
3. Clausing, P., Ann. Physik, (5) 12, 961 (1932).
4. Dawson, J. P., M. S. Thesis, Oklahoma State University (1960).
5. Dushman Equation, See Sears, F. W., and Zemansky, M. W., University Physics Complete, Addison-Wesley Publishing Co., Inc., Reading, Mass., 2d Ed., p 698 (1957).
6. Freeman, R. D., Ph. D. Thesis, Purdue University (1954).
7. Hall, L. D., J. Am. Chem. Soc., 73, 757(1951).
8. Hansen, M., Constitution of Binary Alloys, McGraw-Hill, New York (1958).
9. Harteck, P., Z. physik. Chem., 134, 1(1928).
10. Hempel, W., Z. angew. Chem., 17, 324(1904).
11. Herring and Nichols, Rev Mod Phys. 21, 232(1949).
12. Heydman, W. F., M. S. Thesis, Oklahoma State University (1960).
13. Hildenbrand, D. L., Private Correspondance.
14. Jones, H. A., Langmuir, I., G. E. Rev. 30, 310(1927).
15. Kelley, K. K., U. S. Bur. Mines Bull., 383, (1935).
16. Knudsen, M., Ann. Physik, 29, 179(1909).
17. Michaelson, J. App. Phys., 21, 536(1950).
18. Moisson, H., Compt. rend., 141, 977(1919).
19. Rocco, W. A. and Sears, G. W., Rev. Sci. Instr., 27, 1(1956).
20. Ruff, O. and Bergdahl, G., Z. anorg. Chem., 106, 76(1919).
21. Stull, D. R. and Sinke, G. C., Thermodynamic Properties of the Elements, American Chemical Society, Advances in Chemistry Series No. 18, Washington, 1956.

VITA

James Edward Bennett

Candidate for the Degree of
Master of Science

Thesis: AN ELECTRON BOMBARDMENT FURNACE FOR VAPOR PRESSURE
STUDIES. THE VAPOR PRESSURE OF GOLD

Major Field: Physical Chemistry

Biographical:

Personal Data: Born at Wink, Texas, November 27, 1935,
the son of James G. and L. Leona Bennett.

Education: Graduated from Lamesa High School, Lamesa,
Texas, in 1953; attended Texas A. & M., 1954;
attended Cisco Junior College, Cisco, Texas, 1955;
received the Bachelor of Science degree from
Northwestern State College, Alva, Oklahoma, in
1957, with a major in chemistry; completed the re-
quirements for the Master of Science degree in
May, 1962.